Characterization Testing of Lockheed Martin Standard Micro Pulse Tube Cryocooler

I.M. McKinley, D.L. Johnson, and J.I. Rodriguez

Jet Propulsion Laboratory, California Institute of Technology
Pasadena, CA 91109

ABSTRACT

This paper describes the thermal performance, exported vibration, and magnetics testing and results for a Lockheed Martin standard micro pulse tube cryocooler. The thermal performance of the microcooler was measured in vacuum with heat reject temperatures between 150 and 300 K. The cooler was driven with Thales XPCDE4865 drive electronics for input powers ranging from 4 to 20 W and drive frequency between 84 and 98 Hz. The optimal drive frequency was dependent upon both input power and heat reject temperature. In addition, the exported forces and torques of the cooler were measured with the cooler driven by Thales CDE7232 drive electronics for input powers ranging from 4 to 20 W and drive frequency between 88 and 96 Hz. Moreover, the automatic vibration reduction function of the drive electronics was able to decrease the force along the compressor axis to below 10 mN 0-peak. Finally, the DC and AC magnetic fields around the cooler were measured at various locations.

INTRODUCTION

The Jet Propulsion Laboratory (JPL) has identified the Lockheed Martin standard micro pulse tube cryocooler as a low-cost candidate to provide active cooling on future cost-capped scientific missions. This tactical cooler offers a long lifetime due to the flexure bearings in its compressor and a pulse tube coldhead containing no moving parts. Lockheed Martin has published a number of papers focusing on this cooler in recent years [1, 2, 3, 4]. This cooler has been optimized for a coldtip temperature of 125 K to 150 K and operates with a drive frequency near 100 Hz [2]. In addition, it is capable of operating with a heat rejection temperature below 150 K [3]. This capability is important for deep space missions because of the low survival temperature required for the power savings in survival mode. The compressor weighs 210 grams and the entire cooler weighs 328 grams [3]. Moreover, it has been qualified to a technology readiness level (TRL) 6 [3]. Finally, the cooler tested in this work consisted of physically the same coldhead and compressor as that described in [4] except with a different transfer line. This work seeks to advance the Lockheed Martin standard microcooler towards use in space flight missions by characterizing its thermal performance, exported forces, and electromagnetic interference over a wide range of operating conditions.

Cryocoolers 19, edited by S.D. Miller and R.G. Ross, Jr.

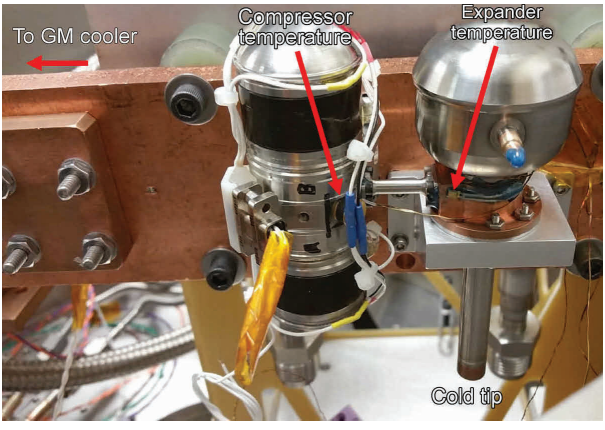

Figure 1. LM cooler in the TVAC test setup. Both the coldblock and MLI are not shown.

THERMAL PERFORMANCE TESTS

Test Setup and Procedure

Figure 1 shows a photograph of the test setup used for thermal performance measurements. The Lockheed Martin (LM) cooler's thermal performance was measured inside a thermal vacuum (TVAC) chamber at JPL's cryocooler characterization facility. Rejection of the LM cooler's heat was achieved by cooling a copper mounting plate with a Gifford-McMahon (GM) laboratory cooler. The cooler heat rejection temperature was defined as the temperature measured on the expander surface. It was maintained between 150 and 300 K with a Lake Shore 340 temperature controller powering Dale resistors. In addition, the compressor temperature was measured and was approximately 5°C warmer than the expander for the duration of the tests. The LM cooler was powered with Thales XPCDE4865 drive electronics supplying between 3.5 and 16 W to the compressor at drive frequencies between 83 and 98 Hz. A coldblock consisting of a copper ring equipped with resistors and a Lake Shore DT670 diode maintained the cold tip temperature between 55 and 225 K by supplying heat loads of between 0 and 2.5 W. Note that all of the cold surfaces inside the vacuum chamber were covered with multi-layer insulation (MLI). In addition, Lockheed Martin provided a recommended maximum drive voltage based on the motor characteristics as a function of frequency, compressor temperature, and current.

Effect of Drive Frequency

Figure 2 shows the specific power of the LM cooler and the motor efficiency vs. drive frequency. The specific power was defined as the compressor input power divided by the cooling power (or coldblock load). The motor efficiency was defined as the quantity of the i^2R losses in the coils subtracted from the compressor input power divided by the compressor input power [5]. In this case, the coil resistance was defined as 5.3 ohms and corresponded to the value at room temperature obtained with a 4-wire measurement. It is evident that the minimum specific power and the maximum motor efficiency both depended on both heat reject temperature and compressor input power. However, for a given heat reject temperature and cooler input power, the respective minimum and maximum fall nearly on the same drive frequency. This indicates that the peak thermodynamic frequency of the coldhead and the compressor resonant frequency are well matched [4].

Effect of Heat Rejection Temperature

Figure 3 shows compressor input power vs. coldblock load (Ross plots) for various expander temperatures with the cooler driven at 96 Hz. It also shows a Ross plot for the 150 K expander tem-

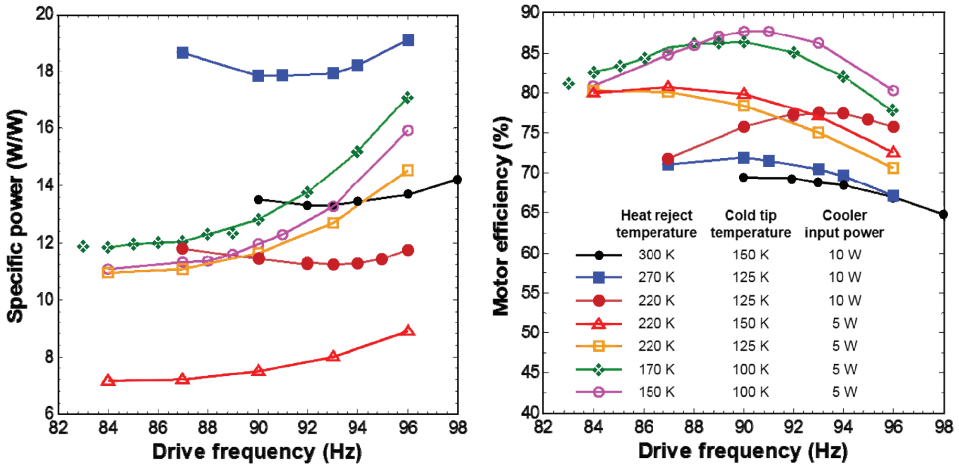

Figure 2. Specific power and motor efficiency vs. drive frequency for various heat rejection (expander) temperatures, cold tip temperatures, and cooler input powers.

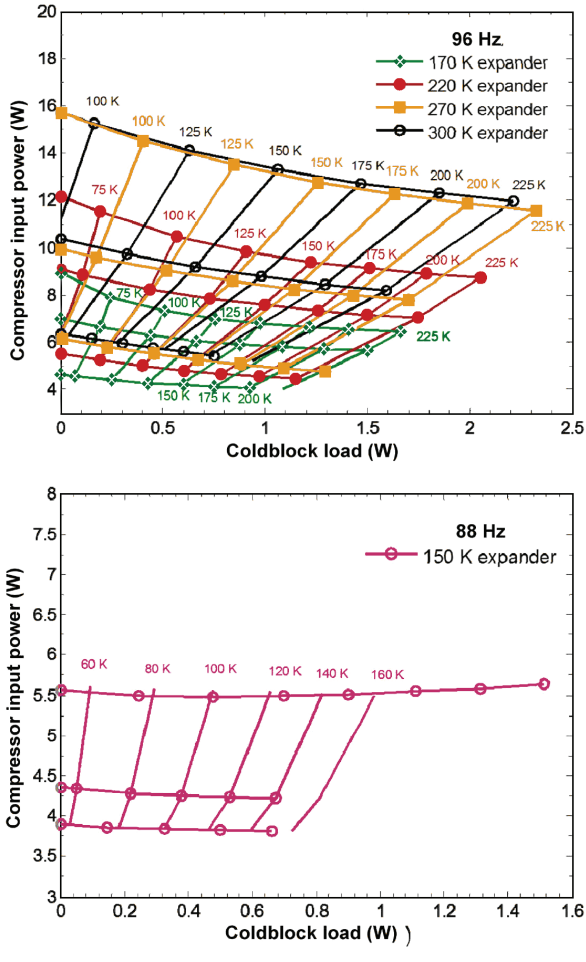

Figure 3. Ross plots for various expander temperatures with the cooler driven at 96 Hz and a Ross plot for 150 K expander temperature with the cooler driven at 88 Hz.

perature with the cooler driven at 88 Hz. Load lines were measured with a fixed compressor input voltage. For a given input voltage, the input power decreased as the cold tip temperature increased. The cold tip temperature for each load line was fit as a function of both compressor input power and coldblock load. These fits were used to obtain the isotherms shown in Figure 3. For a given cold tip temperature and input power, the cooling capability of the cooler increased with decreasing expander temperature. Note that the compressor input power was limited to 16 W for the duration of these tests. The maximum input power was not necessarily reached during these tests. In fact, Lockheed Martin has input up to 20 W to this model cooler at 300 K expander temperature for cold tip temperatures up to 200 K corresponding to 2.25 W of cooling [2].

EXPORTED FORCES AND TORQUES

Test setup and Procedure

Figure 4 shows a photograph of the LM cooler mounted on a Kistler dynamometer that measured exported forces from the cooler. It also shows the coldblock previously described. The complete test setup has been described in the literature previously [6, 7]. The cooler was operated with the Thales CDE7232 drive electronics for compressor input powers ranging from 5 to 18 W and drive frequency ranging from 88 to 96 Hz. In addition, the automatic vibration reduction (AVR) feature of this drive electronics was tested. Similar to previous works, the force signal in the compressor axis was used as feedback for this feature [6, 7]. The expander temperature of the cooler was not actively controlled but did not exceed 30°C for the duration of these tests. In addition, the cold tip was not contained in a vacuum housing during these measurements. Also note that the compressor mount was not bonded to the compressor when it was delivered to JPL and for the entire duration of the thermal performance and electromagnetic interference tests. However, the mount was bonded to the compressor with Nusil CV-2946 for the duration of the exported force results presented here.

Effect of Drive Frequency

Figure 5 shows the 0-peak force vs. harmonic in all three axes for 10 and 15 W compressor input power for drive frequency between 88 and 96 Hz. Note that harmonic 0 corresponded to the drive frequency. The compressor axis force at the drive frequency decreased with decreasing frequency. In most cases, the force for a given harmonic, direction, and input power decreased with decreasing drive frequency. In addition, the fourth harmonic of the force in the transfer line axis was largest among the harmonics. The fourth harmonic in the vertical axis at 15 W input power was also very large. This possibly could be attributed to non-uniform magnetic materials in the compressor or small motor misalignment. Indeed, magnetic analysis performed by Lockheed Martin indicated that non-uniform magnetic side loads could lead to lateral forces at the higher harmonics. However, it should be noted that the jitter introduced by large forces at higher harmonics is significantly less than that due to smaller harmonics. For example, 2 N at 400 Hz leads to the same displacement as 0.02 N at 40 Hz.

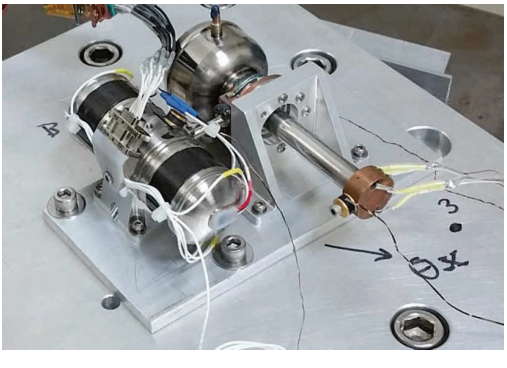

Figure 4. Photograph of the LM cooler mounted on the Kistler dynamometer.

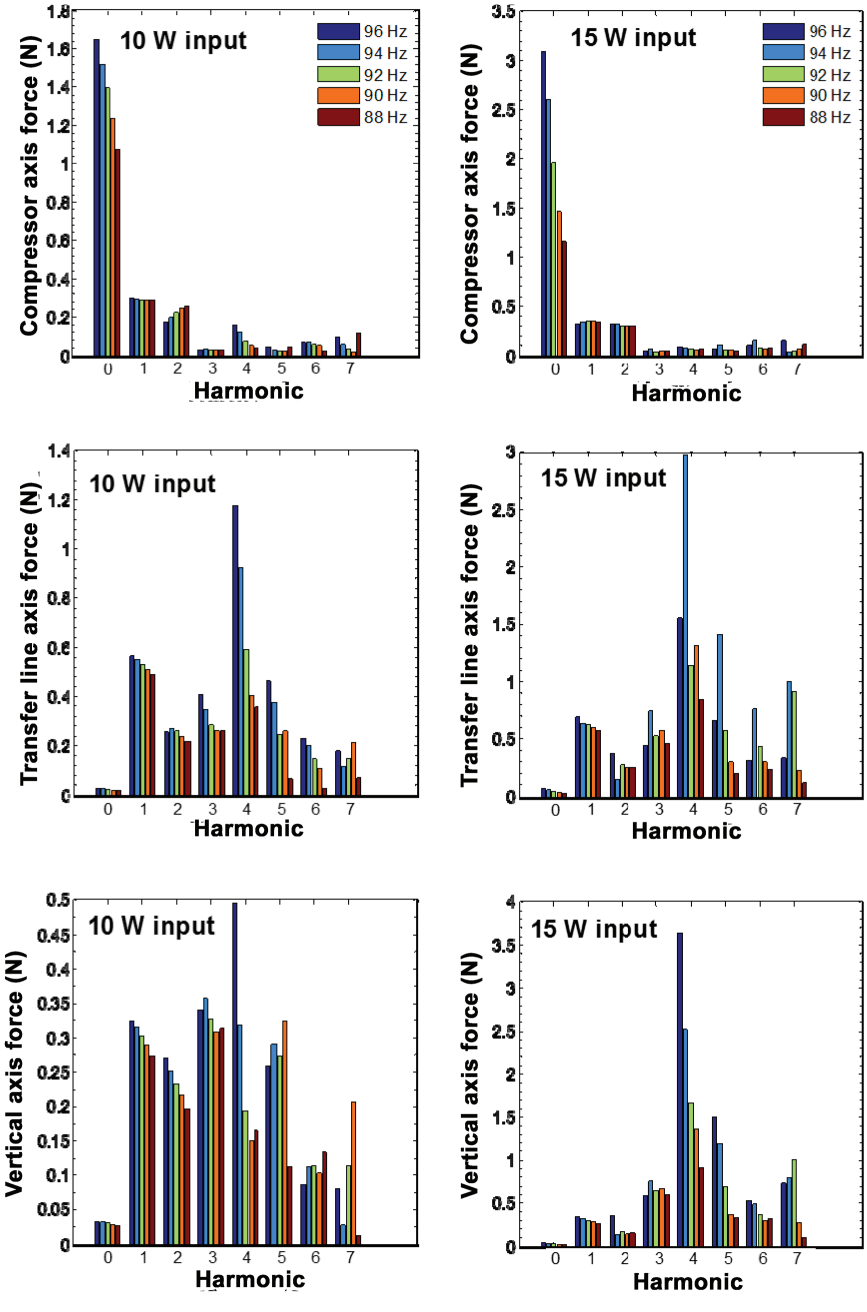

Figure 5. Force vs. harmonic in all three axes for 10 and 15 W compressor input power for drive frequency between 88 and 96 Hz. Note the vertical upper limit is different on each plot.

Effect of Input Power

Figure 6 shows the force vs. harmonic in all three axes for various input voltages as well as the same data as force vs. compressor input power for various harmonics with the cooler driven at 96 Hz. It is evident that for a given harmonic and axis, the force decreased with decreasing input

power/voltage. In addition, the majority of the compressor axis force was contained in the drive frequency. However, the fourth harmonic of the transfer line and vertical axis forces was the largest. The transfer line axis force was the smallest reaching a peak of 1.6 N 0-peak. Moreover, the vertical axis force exceeded that of the compressor axis for input voltages above 11 V_{rms}. In fact, there was a sharp increase in vertical axis force for input voltages above 10 V_{rms} and the cooler compressor

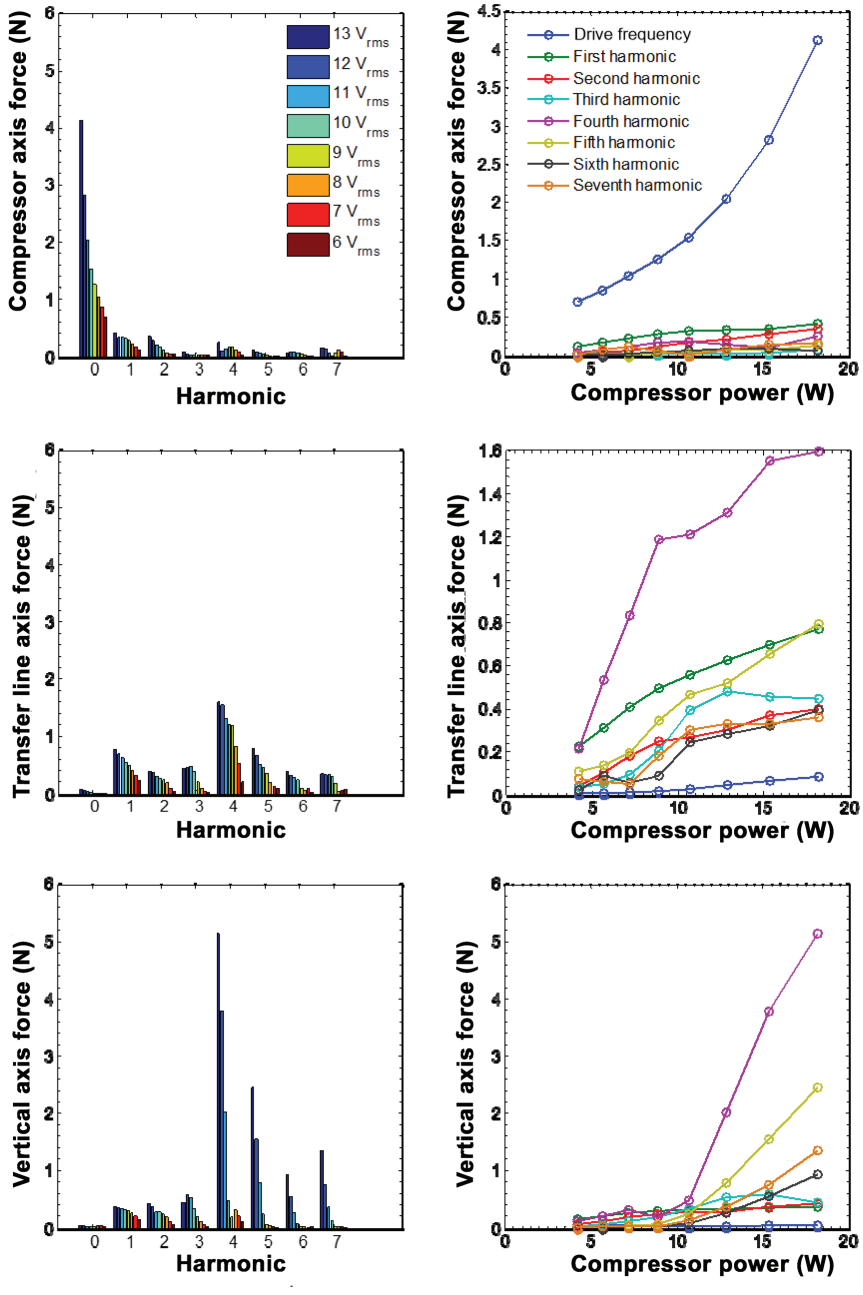

Figure 6. Force vs. harmonic in all three axes for various input voltages as well as force vs. compressor input power in all three axes for various harmonics. The cooler was driven at 96 Hz in all cases without AVR. The data in the left and right columns is the same. Note the vertical upper limit is different for each plot in the right column.

made a louder noise at a different tone. Again, the large forces in the vertical axis could possibly be attributed to non-uniform magnetic side loads in the compressor.

Effect of Automatic Vibration Reduction

Figure 7 shows the force in the compressor axis as a function of harmonic for various input voltages at 96 Hz with the automatic vibration reduction function of the drive electronics off and on. The AVR function was able to reduce the first four harmonics of the compressor axis force to below 10 mN 0-peak for input voltages up to 11 V_{rms}. For voltages above 11 V_{rms}, the function was not able to complete its calibration period and continuously changed the input wave forms to the compressor motors.

ELECTROMAGETIC INTERFERENCE

DC measurements

Figure 8 (left) shows the test setup used to measure the DC magnetic fields surrounding the LM cooler. The cooler was without any mechanical supports/mounting structures. A Lake Shore 475 DSP Gaussmeter with a Lake Shore HMMA-1808-VF axial probe was used to measure the DC field in the axial and radial directions. An axial position of 50 cm corresponded to the center of the compressor. Figure 9 (left) shows the magnitude of the magnetic field as a function of axial position at a radial distance of 7 cm from the edge of the compressor. The magnitude of the field was determined by taking the square root of the sum of the squares of the radial and axial measurements at

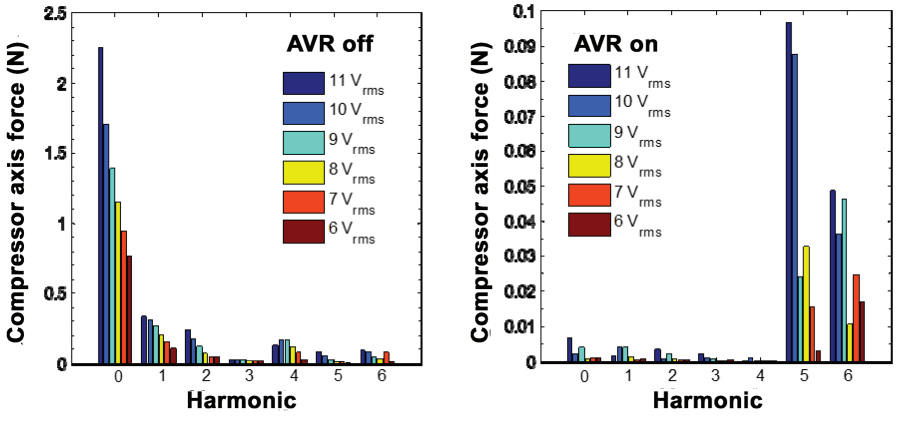

Figure 7. Force in the compressor axis vs. harmonic for various input voltages at 96 Hz with AVR off and on. Note the vertical upper limit is different on each plot.

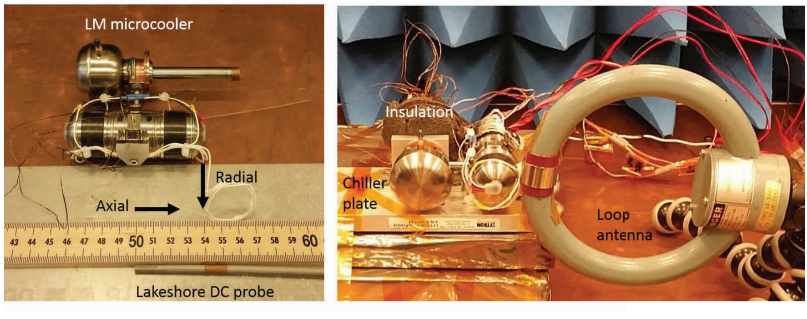

Figure 8. Photographs of the test setup for DC (left) and AC (right) magnetic field measurements.

a given location. Note that the magnetic field of the Earth was subtracted from the measured field. Figure 9 (right) shows the axial magnetic field as a function of distance from the compressor end at the radial center of the compressor. In this case, the radial component of the field was equal to zero. Figure 9 (right) indicates the expected 1/distance^3 relationship between DC field of a permanent magnet and distance from it [8]. In addition, magnetic mapping was performed around one rotational axis and additional measurements were taken about multiple rotational axes in order to establish the magnetic dipole moment of the cooler. The magnetic mapping yielded a quadrupole magnetic field of 14.41 nT pk-pk at a distance of 1 m. This was a result of the compressor containing more than one magnet. The overall magnetic dipole moment was calculated from the measurements about multiple rotational axes and was 9.18 mA-m^2. Finally, the magnetic dipole field was calculated from the dipole moment and was 3.67 nT pk-pk at 1 m.

AC measurements

Figure 8 (right) shows the test setup used to measure the AC magnetic fields surrounding the LM cooler. The cooler was mounted on a chiller plate that was used to maintain the expander at room temperature while the cooler operated. Insulation was placed around the cold tip to reduce the buildup of ice. The cooler was operated at input powers between 10 and 20.5 W at 96 Hz. The AC magnetic field was measured as a function of frequency in the radial and axial directions at various locations using a Singer 94605-1 loop antenna connected to a Rohde & Schwarz ESIB40 spectrum analyzer. Peaks in the AC field vs. frequency occurred at the drive frequency and its higher harmonics. The magnitude of the magnetic field at the drive frequency and first harmonic (96 and 192 Hz) were calculated by taking the square root of the sum of the squares of the axial and radial components. For a given radial distance, the magnitude of the field was nearly independent of axial location along the compressor. In addition, for a given location, the magnitude of the field was weakly dependent on cooler input power and varied by less than 5% for cooler input power ranging from 10 W to 20.5 W. Figure 10 shows the magnitude of the AC magnetic field at 96 Hz and 192 Hz as a function of axial distance at from the center of the compressor end (left) and of radial distance from the center of the compressor edge (right). The magnitude of the AC field decreased with increasing distance from the compressor. The Military Standard RE101 requirement [9] was met at 7 cm from the compressor end for both Army and Navy applications. However, it was not met 7 cm radially from the side of the compressor for Navy applications. These results indicate that the cooler would need magnetic shielding to meet the RE101 requirement for Navy applications.

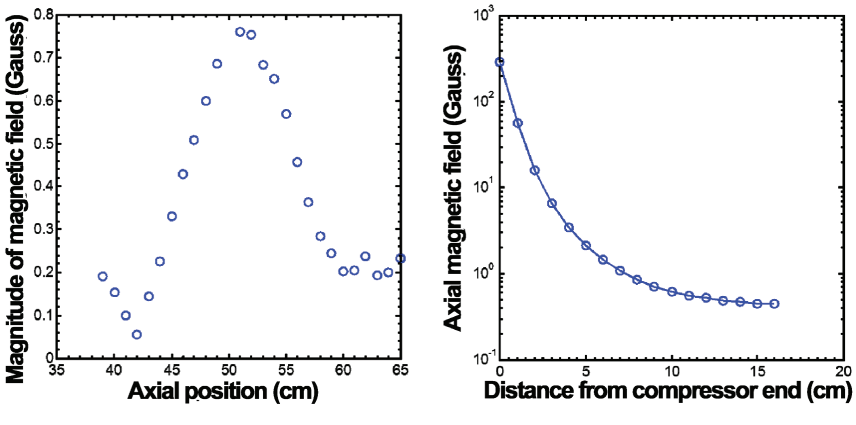

Figure 9. The magnitude of the DC magnetic field as a function of axial position at a radial distance of 7 cm from the compressor edge (left) and axial magnetic field on axis as a function of the distance from the

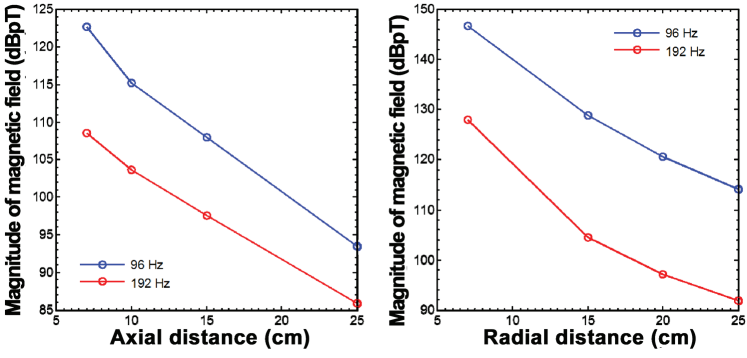

Figure 10. The magnitude of the AC magnetic field for the operating LM cooler as a function of axial distance from the compressor end (left) and as a function of radial distance from the compressor edge at the

CONCLUSION

This paper described the thermal performance, exported vibration, and magnetics testing and results of a Lockheed Martin standard micro pulse tube cryocooler. The thermal performance of the microcooler driven with Thales XPCDE4865 drive electronics was reported for heat reject temperatures between 150 and 300 K, input powers ranging from 4 to 20 W, and drive frequency between 84 and 98 Hz. The optimal drive frequency was dependent on both input power and heat reject temperature. In addition, the exported forces and torques of the cooler were measured with the cooler driven by Thales CDE7232 drive electronics for input powers ranging from 4 to 20 W and drive frequency between 88 and 96 Hz. The exported forces were dependent on both input power and drive frequency. Furthermore, the automatic vibration reduction function of the drive electronics was able to decrease the force in the compressor axis to below 10 mN 0-peak for input power up to approximately 12 W. Finally, the DC and AC magnetic fields around the cooler were measured at various locations. The DC measurements revealed the cooler to have a magnetic dipole field of 3.67 nT pk-pk at a distance of 1 m. The AC measurements revealed that the cooler did not meet the RE101 requirement at a distance of 7 cm for Navy applications. Overall, this cooler remains an excellent candidate for future space missions.

ACKNOWLEDGMENT

The work described in this paper was carried out at the Jet Propulsion Laboratory, California Institute of Technology, and was sponsored by the NASA Science Mission Directorate, Maturation of Instruments for Solar System Exploration (MatISSE) program. In addition, the authors would like to acknowledge Jeff Olson, Evan Droz, Andy Lamborn, Jerry Gutierrez, Katherine Dang, Pablo Narvaez, and Diana Blayney for their contributions to this work.

REFERENCES

1. J. Olson, P. Champagne, E. Roth, T. Nast, E. Saito, V. Loung, A. Kenton and C. Dobbins, “Microcryocooler for tactical and space applications,” *Adv. in Cryogenic Engineering*, Vol. 59, Amer. Institute of Physics, Melville, NY (2014).
2. J. Olson, P. Champagne, E. Roth, G. Kaldas, T. Nast, E. Saito, V. Loung, B. McCay, A. Kenton and C. Dobbins, “Coaxial Pulse Tube Microcryocooler,” *Cryocoolers 18*, ICC Press, Boulder, CO (2015).
3. T. Nast, E. Roth, J. Olson, P. Champagne and D. Frank, “Qualification of Lockheed Martin micro pulse tube cryocooler to TRL6,” *Cryocoolers 18*, ICC Press, Boulder, CO (2015).
4. J. Olson, G. Kaldas, P. Champagne, E. Roth and T. Nast, “MatISSE Microcryocooler,” in *IOP Conf. Series: Materials Science and Engineering 101*, 2015.

5. A. Orlowska and G. Davey, “Measurement of losses in a Stirling cycle cooler,” *Cryogenics,* vol. 27, no. 11, pp. 645-651, 1987.

6. D. Johnson, I. McKinley, J. Rodriguez, B. Carroll and H. Tseng, “Characterization testing of the Thales LPT9310 pulse tube cryocooler,” *Cryocoolers 18*, ICC Press, Boulder, CO (2015).

7. D. Johnson, I. McKinley and J. Rodriguez, “Flight Qualification Testing of the Thales LPT9510 Pulse Tube Cooler,” *Cryocoolers 18*, ICC Press, Boulder, CO (2015).

8. R. Weidner and R. Sells, *Elementary Classical Physics Volume 2: Electromagnetism and Wave Motion*, Allyn and Bacon, Inc., Boston, MA 1965.

9. Department of Defense, “Requirement for the Control of Electromagnetic Interference Characteristics of Subsystems and Equipment,” 2015.